Specific neural substrate linking respiration to locomotion

Jean-François Gariépy[a], Kianoush Missaghi[b], Stéphanie Chevallier[a], Shannon Chartré[b], Maxime Robert[b], François Auclair[a], James P. Lund[a,c,1], and Réjean Dubuc[a,b,2]

[a]Central Nervous System Research Group, Department of Physiology, Université de Montréal, Montréal, QC, Canada H3T 1J4; [b]Research Group in Adapted Physical Activity, Department of Kinesiology, Université du Québec à Montréal, Montréal, QC, Canada H2X 1Y4; and [c]Faculty of Dentistry, McGill University, Montréal, QC, Canada H3A 2B2

Edited by Sten Grillner, Karolinska Institutet, Stockholm, Sweden, and approved November 22, 2011 (received for review August 10, 2011)

When animals move, respiration increases to adapt for increased energy demands; the underlying mechanisms are still not understood. We investigated the neural substrates underlying the respiratory changes in relation to movement in lampreys. We showed that respiration increases following stimulation of the mesencephalic locomotor region (MLR) in an in vitro isolated preparation, an effect that persists in the absence of the spinal cord and caudal brainstem. By using electrophysiological and anatomical techniques, including whole-cell patch recordings, we identified a subset of neurons located in the dorsal MLR that send direct inputs to neurons in the respiratory generator. In semi-intact preparations, blockade of this region with 6-cyano-7-nitroquinoxaline-2,3-dione and (2R)-amino-5-phosphonovaleric acid greatly reduced the respiratory increases without affecting the locomotor movements. These results show that neurons in the respiratory generator receive direct glutamatergic connections from the MLR and that a subpopulation of MLR neurons plays a key role in the respiratory changes linked to movement.

breathing | modulation | motor output | exercise | brainstem

At the onset of exercise in humans, ventilation increases abruptly. Further increases occur during the exercise bout and these changes are correlated with the intensity of the motor output (1). Chemoreception was proposed to induce these changes, as breathing air with high partial pressure of CO_2 was known to markedly increase respiration (2, 3). However, it was later demonstrated in several animal species that the CO_2 arterial partial pressure does not increase during moderate exercise, and it even decreases (2). Other substances such as O_2, H^+ ions, and S-nitrosothiols are also known to modulate respiration (4–6), but there are not sufficient changes in these respiratory modulators to explain the respiratory increases during exercise (2, 7).

Alternatively, neural mechanisms have been proposed to contribute to the respiratory changes during exercise. For instance, sensory feedback from the contracting muscles could play a role (8, 9). However, respiratory increases also occur during mental simulation of movement as well as before the onset of exercise in humans (10, 11). Furthermore, it was shown that the stimulation of the forebrain and brainstem regions controlling locomotion increases respiratory activity in the absence of movement-related feedback in animal models (12–14). These results indicate that a neural feedback mechanism cannot be solely responsible for movement-related increases in respiratory activity; central connections between locomotor and respiratory areas in the brain are likely to play an important role (15). However, because the central neural connections were never identified, this central hypothesis remains criticized (16). For instance, whether the respiratory increases rely on direct projections from the brainstem locomotor centers or on feedback from other parts of the locomotor networks such as the spinal cord remains undetermined.

The characterization of the neural mechanisms underlying the generation and modulation of respiration has advanced considerably as a result of newly developed in vitro mammalian preparations (17–26). Moreover, many identified brainstem neurons such as serotoninergic neurons, locus coeruleus neurons, and orexin neurons modulate breathing in accordance with behavioral states or CO_2 levels (27–29). However, the role of these modulatory mechanisms in the respiratory increases related to exercise is unknown. In this study, we used the in vitro brainstem–spinal cord preparation of the lamprey, in which it is possible to simultaneously assess locomotor and respiratory outputs while recording individual neurons in the neural networks controlling locomotion and respiration. The pre-Bötzinger complex is a medullary region critical for the generation of respiratory activity in mammals (30, 31). The lamprey respiratory generator is localized in a region of the pons (32) referred to as the paratrigeminal respiratory group (pTRG) (33), which presents pharmacological similarities with the pre-Bötzinger complex of mammals (34, 35). The neural centers controlling locomotion in lampreys have been very well documented (36–38). One such locomotor center is the mesencephalic locomotor region (MLR), located at the mesopontine border. It was shown to initiate and control the intensity of locomotion in a graded fashion (36), similarly to what was previously shown in mammals (39). It is thought to have a similar function in humans (40). By using kinematic, anatomical, and electrophysiological (Fig. S1) approaches, we show that a group of neurons located in the dorsal part of the MLR projects to neurons in the pTRG. Blocking the dorsal part of the MLR abolishes an important part of the respiratory changes linked to exercise. Our results suggest that a major part of the respiratory increases rely on a neural command emerging from a specific group of neurons in the MLR.

Results

We first observed the respiratory changes that occur in relation to movements in freely behaving lampreys (Fig. 1*A*; raw data provided in Fig. S2). Respiratory increases were found to occur before the onset of movement (increase by 10.4 ± 10.0%; 1.55 ± 0.30 Hz vs. 1.42 ± 0.38 Hz in control; one-tailed paired *t* test, $P < 0.05$; $n = 9$, locomotor bouts; measured 6 s before movement) and became more important during movement (2.09 ± 0.48 Hz; one-tailed paired *t* test, $P < 0.001$; $n = 9$ locomotor bouts). These results reproduce well what was previously shown in mammals (10–14). We then isolated the brainstem and spinal cord in vitro to see whether feedback from the contracting muscles was necessary for the respiratory increases (Fig. 1 *B*, *B′*, and *C*). Similarly to what was shown

Author contributions: J.-F.G., J.P.L., and R.D. designed research; J.-F.G., K.M., S. Chevallier, S. Chartré, M.R., F.A., and R.D. performed research; J.-F.G., K.M., S. Chevallier, F.A., and R.D. analyzed data; and J.-F.G., K.M., J.P.L., and R.D. wrote the paper.

The authors declare no conflict of interest.

This article is a PNAS Direct Submission.

[1]Deceased December 8, 2009.

[2]To whom correspondence should be addressed. E-mail: rejean.dubuc@gmail.com.

See Author Summary on page 365.

This article contains supporting information online at www.pnas.org/lookup/suppl/doi:10.1073/pnas.1113002109/-/DCSupplemental.

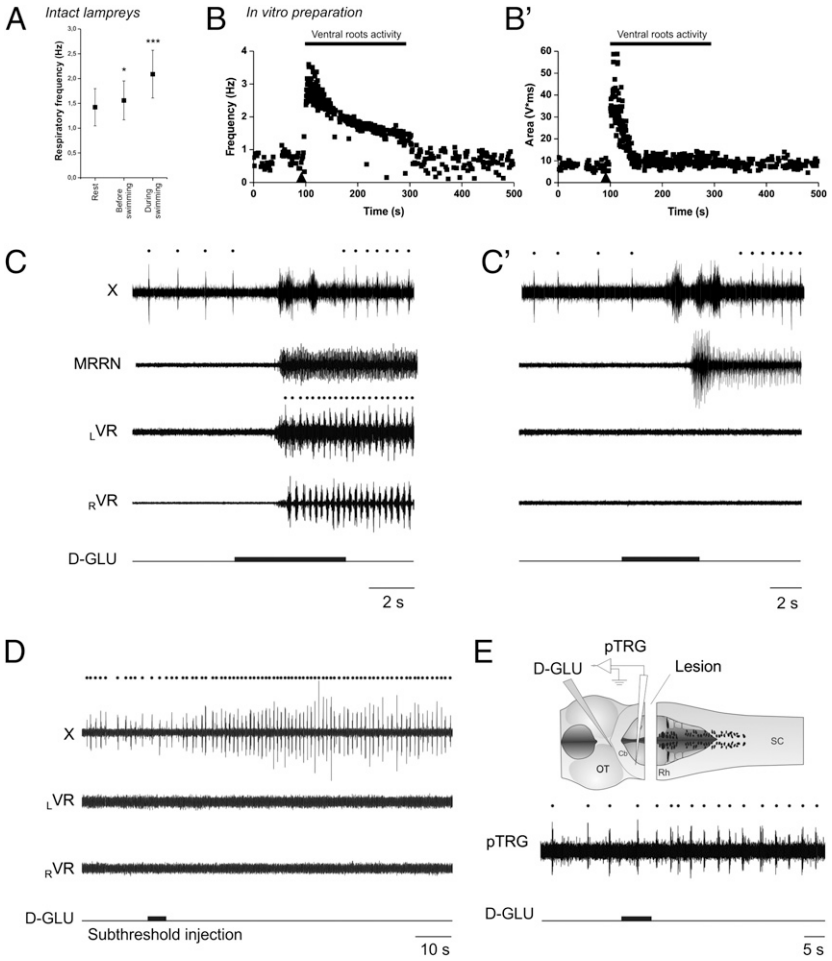

Fig. 1. Respiratory increases related to locomotion in vivo and in vitro. (*A*) Analysis of the respiratory frequency at rest, 6 s before swimming, and during swimming in vivo. Analyses were made for a total of nine locomotor bouts in six animals. Raw traces are provided in Fig. S2. (*B* and *B′*) Time course of the instantaneous frequency (*B*) and area (*B′*) of the respiratory bursts recorded from the vagal motoneuronal pool during fictive locomotion in the in vitro brainstem–spinal cord preparation. Triangle marks the beginning of D-glutamate injection in the MLR, which lasted 5 s. Raw traces for this fictive locomotor bout are provided in Fig. S3. (*C*) Raw traces of the respiratory increases following D-glutamate (D-GLU, 2.5 mM) in the MLR in a control brainstem–spinal cord preparation. (*C′*) Similar D-glutamate injection after removal of the spinal cord in the same preparation. In the absence of the spinal cord, the activity of the brainstem locomotor networks is monitored with an extracellular recording electrode placed over reticulospinal cells in the MRRN. (*D*) Effects of a D-glutamate MLR injection that was not large enough to elicit locomotor activity in a control brainstem–spinal cord preparation. Note that the increases in respiratory frequency remained even though the stimulation was not sufficiently strong to induce locomotion on the ventral roots. (*E*) Effects of MLR stimulation on respiratory frequency after removing the caudal half of the rhombencephalon. Dots indicate respiratory and locomotor cycles. X, vagal motor nucleus; $_{L}$VR, left ventral root; $_{R}$VR, right ventral root; SC, spinal cord; OT, optic tectum; Cb, cerebellar commissure; Rh, rhombencephalon. MRRN, middle rhombencephalic reticular nucleus.

in mammals (12–14), we found that chemical stimulation of the MLR by D-glutamate (2.5 mM) injections induces fictive locomotor activity, as recorded from the ventral roots, along with increases in respiration, despite the absence of feedback from the muscles. Respiratory frequency was increased by 91.4 ± 58.6% (0.89 ± 0.30 Hz in control to 1.57 ± 0.39 Hz; one-tailed paired *t* test, $P < 0.001$; $n = 7$ animals, $n = 48$ locomotor bouts; Fig. S3 and *SI Text*). We also found that stimulation of the MLR with smaller injections of D-glutamate could induce respiratory changes without triggering locomotor activity (Fig. 1*D*). In these cases, the spread of the injections did not exceed 50 μm in diameter compared with 300 μm for the control injections (*Materials and Methods*). These results suggest a strong link between the locomotor and respiratory control networks that could operate in the absence of locomotor output; further experiments were carried out to identify the underlying neural substrate.

Localization of Neural Connections Underlying Respiratory Changes. To test whether feedback from spinal locomotor networks was involved in the respiratory increases, the spinal cord was transected at the level of the obex in three animals. After removal of the spinal cord, stimulation of the MLR still induced similar increases in respiratory activity (control, increases of 116.8 ± 76.8%, $n = 17$ D-glutamate injections; transected, 120.6 ± 79.0%, $n = 21$ D-glutamate injections; two-tailed *t* test, $P = 0.88$; Fig. 1 *C* and *C′*). Furthermore, removing all brainstem tissue caudal to the trigeminal motor nuclei ($n = 3$ preparations, $n = 28$ injections; Fig. 1*E*) did not prevent the respiratory changes in response to MLR stimulation. The respiratory rhythm recorded from the pTRG still increased by 68.7 ± 40.0% in response to MLR stimulation (0.28 ± 0.05 Hz in control, 0.48 ± 0.11 Hz after stimulation; one-tailed paired *t* test, $P < 0.001$; $n = 28$ injections). Although these respiratory increases were still important, they were statistically smaller than those occurring in control condition ($P < 0.01$). It is noteworthy that the respiratory frequency was generally slower in the absence of the spinal cord and caudal brainstem; thus, the increases could only be compared in

relative terms (i.e., as percentages). This reduction suggests that the respiratory generator receives an excitatory drive from neural areas located caudal to the trigeminal motor nucleus. Overall, the results from the lesion experiments suggest that an important part of the neural circuitry responsible for respiratory changes following MLR stimulation is located in the rostral part of the hindbrain.

Underlying Neural Connectivity. To further characterize the connections between the MLR and respiratory neurons, we recorded the synaptic responses of respiratory motoneurons to MLR stimulation (n = 24 preparations; single pulses, 2 ms duration; Fig. 2). In four of these experiments, intracellular recordings of respiratory motoneurons were made on both sides of the brainstem. The size of the area of excitatory postsynaptic potentials (EPSPs) was well correlated with the MLR stimulation intensity (r = 0.81 ± 0.08; linear fits; $P < 0.001$ for each preparation and each side; n = 627 ipsilateral EPSPs; n = 705 contralateral EPSPs; Fig. 2 *A* and *B*). The latency of the synaptic responses was significantly shorter in motoneurons recorded on the ipsilateral side of the MLR (10.0 ± 4.8 ms, n = 4 ipsilateral motoneurons; contralateral, 17.1 ± 7.4 ms, n = 4 contralateral motoneurons; one-tailed paired t test, $P < 0.05$).

Glutamatergic receptor blockers [6-cyano-7-nitroquinoxaline-2,3-dione (CNQX) and (2R)-amino-5-phosphonovaleric acid (AP5); n = 5 preparations, n = 5 cells] were injected in the pTRG to determine if it acted as a relay for MLR inputs to respiratory motoneurons (Fig. 2*C*). Bilateral injections of CNQX (1 mM) and AP5 (500 μM) in the pTRG significantly reduced the area of EPSPs (reduction of 67.2 ± 10.0%; one-tailed paired t test; n = 5 motoneurons; $P < 0.001$). After washout, the area of EPSPs partially recovered (67.6 ± 22.2% of control; one-tailed paired t tests; n = 5 motoneurons; $P < 0.05$). These results suggest that there are synaptic connections between the MLR and the respiratory generator. Blocking the pTRG did not completely abolish the motoneuronal EPSPs, suggesting that monosynaptic connections from the MLR to the respiratory motoneurons could also be present. To further confirm that the MLR connects to the respiratory central pattern generator (CPG), we performed trains of electrical stimulation in the MLR. We found that this induced resets of the respiratory rhythm (Fig. S4).

Detailed Connectivity Between MLR Neurons and Respiratory Generator. The preceding physiological experiments suggested that connections between the MLR and the respiratory CPG were present. Whether these connections were direct was not established, and we addressed this question by using whole-cell patch recordings of MLR and pTRG neurons. The first series of experiments consisted in recording from MLR cells. Dextran amines were injected in the IX nucleus and the pTRG (Fig. S5) to label MLR cells that projected to the respiratory centers, and single MLR cells were targeted for patch recordings (n = 8 cells, n = 8 preparations). The posterior tuberculum (PT) is part of the supraspinal system controlling locomotion in lampreys and constitutes a powerful input to the MLR. It was shown to be a relay involved in the transformation of olfactory inputs into locomotor commands (41), and we used it to trigger activation of the brainstem locomotor networks. The PT was stimulated (5–10 μA; 3 Hz; 2-ms pulse duration; 10 s) and excitatory currents were induced in the MLR cells, concomitantly to middle rhombencephalic reticular nucleus (MRRN) activity, as would be expected for neurons activated during locomotion (Fig. 3*A*). The PT was also stimulated with single pulses at stronger intensities (10–15 μA) and short-latency excitatory postsynaptic currents (EPSCs) were elicited in MLR neurons (Fig. 3*B*). After the recorded MLR neurons were filled with biocytin, their axonal projections were examined and fibers were seen in the pTRG on both sides (Fig. 3*C*). The eight labeled neurons had a very similar projection pattern. They typically sent one to three major branches ipsilaterally and one major axonal branch contralaterally that divided into smaller branches with varicosities. Interestingly, all cells sent varicosed fibers in the pTRG, with some fibers reaching the respiratory motoneurons nuclei on both sides (Fig. 3 *E–G*). Some varicosities were observed in close proximity to pTRG neurons that had also been retrogradely labeled from injections in the respiratory motoneuronal pools (Fig. 3*H*). Interestingly, none of the MLR cells had significant axonal projections within the hindbrain reticular nuclei, known to relay locomotor commands to the spinal cord (36–38). To address this point further, fluorescent dextran amines were injected in the reticular formation and in the respiratory motor nuclei to label cells that would project to both structures. There were no double-labeled cells in the MLR, suggesting that separate populations of MLR neurons project to locomotor and respiratory structures. We found that MLR neurons projecting to the respiratory motor nuclei were generally located in the dorsal part of the MLR, whereas those projecting to the reticular formation were located more ventrally (Fig. 3*D*).

We then examined the responses of neurons within the respiratory generator to MLR stimulation. We focused on pTRG neurons projecting to the respiratory motoneurons by first injecting dextran amines into the IX motor nucleus on one side. This allowed us to target pTRG neurons for whole-cell patch

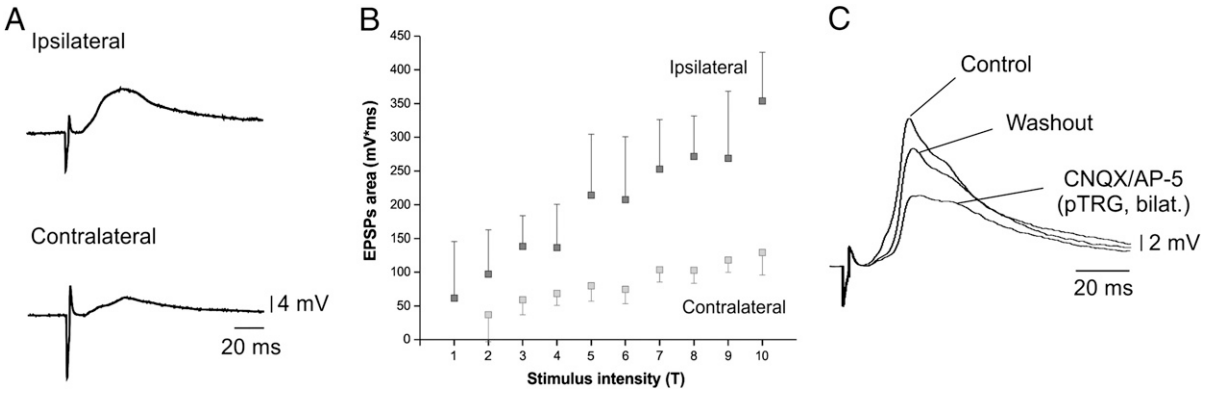

Fig. 2. EPSPs induced in respiratory motoneurons by MLR stimulation. (*A*) Average EPSPs (10 traces) evoked in respiratory motoneurons located ipsilaterally and contralaterally to the stimulated MLR (2-ms pulse duration, 12 μA). (*B*) Plot of the area of EPSPs vs. the MLR stimulation intensity. The intensity of MLR stimulation was varied from threshold (T) level (1T) to 10 times threshold. (*C*) EPSPs recorded in respiratory motoneurons following MLR stimulation under control condition and after localized injection of CNQX and AP5 bilaterally in the pTRG.

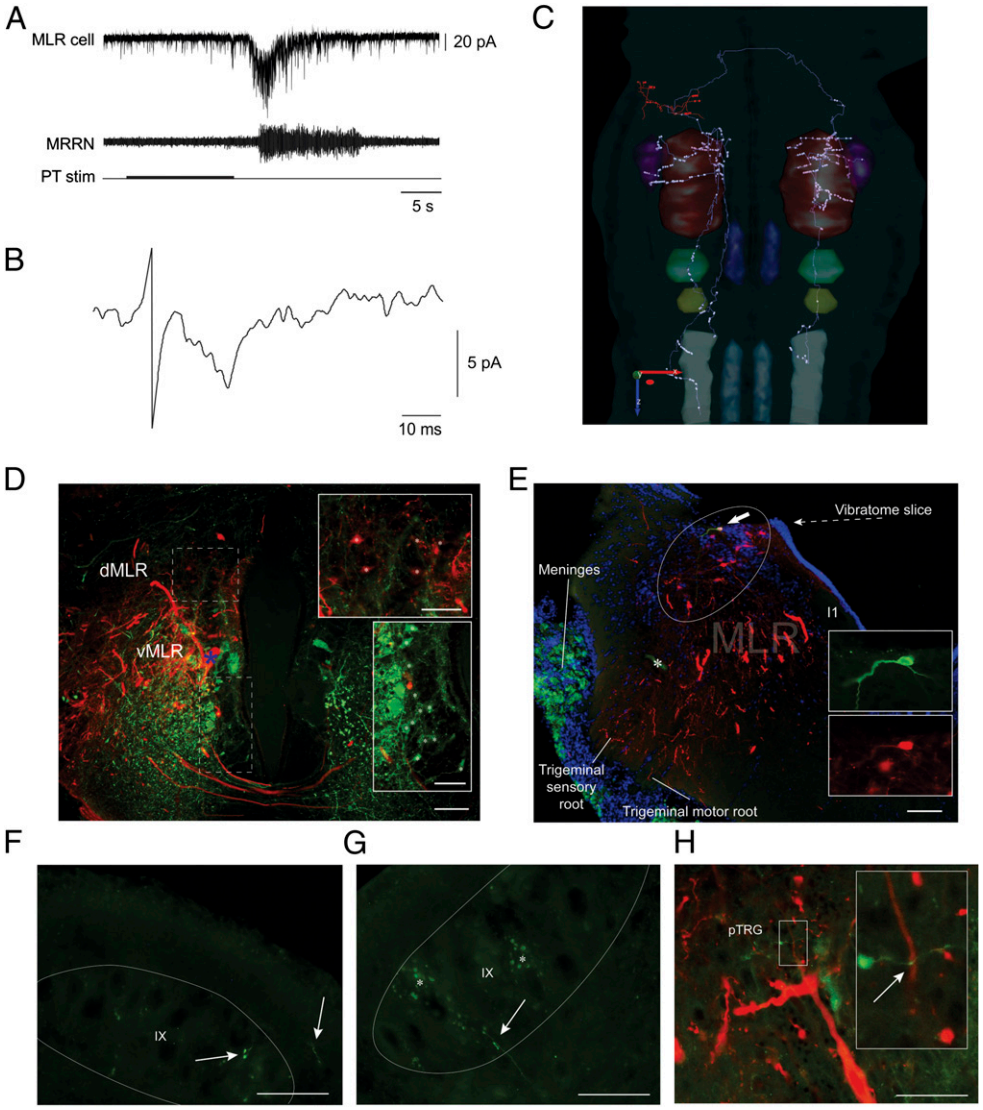

Fig. 3. Electrophysiological and anatomical characterization of individual MLR neurons projecting to the respiratory nuclei. (*A*) Electrophysiological recordings of a single neuron in the MLR in voltage-clamp whole-cell mode following stimulation of the PT. (*B*) Short latency EPSCs (average of 10 traces) evoked by PT stimulation. (*C*) Three-dimensional reconstruction of the axonal projections of the recorded neuron seen from a dorsal view. Varicosities and dendritic spines are represented as circles. The diameter of the axons, dendrites, and cell body were amplified for better visibility. The *y*-, *z*-, and *x*-axis scales represent 500 μm. Color correspondence: dendrites and cell body, light red; axons, light grey; V, dark red; VII, light green, IX, dark yellow; X, dark grey; MRRN, dark blue; PRRN, light blue; pTRG, purple. (*D*) Superimposition of photomicrographs illustrating the populations of MLR neurons backfilled from injections in the respiratory motoneurons (red) and in the reticular formation (green). The dorsal (dMLR) and ventral (vMLR) parts of the MLR are indicated. The asterisk marks a reticulospinal cell that was labeled by the respiratory motoneuron injection. White asterisks (*Insets*) indicate MLR neurons. (Scale bars: 100 μm; *Insets*, 50 μm.) (*E*) Superimposition of three photomicrographs illustrating the whole-cell patch-recorded neuron intracellularly labeled with biocytin (green) among a population of other MLR neurons projecting to the respiratory motor nuclei (dextran amines, red) as seen on a cross section at the level of the MLR. DAPI labeling (blue) shows the location of DNA-containing cell nuclei in the region. I1 is a giant reticulospinal cell used as an anatomical landmark for the position of the MLR. Asterisk marks artifact of tissue folding. (Scale bar: 100 μm.) (*F*) Photomicrograph illustrating two axonal branches (arrows) from the labeled MLR neuron in the ipsilateral IX. (Scale bar: 50 μm.) (*G*) Photomicrograph illustrating an axonal branch (arrow) from the labeled MLR cell in the contralateral IX motor nucleus. Asterisk marks autofluorescent globular artifacts. (Scale bar: 50 μm.) (*H*) Photomicrographs illustrating an axonal branch coming from the MLR cell in the contralateral pTRG. A varicosity (arrow) can be seen in close proximity with a dendrite from a retrogradely labeled pTRG neuron (red). The larger photograph was taken under standard epifluorescence microscopy. *Inset*: Photomicrograph obtained with an Olympus FV1000 confocal microscope equipped with a 60× objective (oil, NA = 1.42). The photograph is a superimposition of two consecutive 0.5-μm optical slices taken from a *z*-stack of 14 photographs. (Scale bar: 50 μm.) PRRN, posterior rhombencephalic reticular nucleus; MRRN, middle rhombencephalic reticular nucleus; PT, posterior tuberculum; pTRG, paratrigeminal respiratory group; V, trigeminal motor nucleus; VII, facial motor nucleus; IX, glossopharyngeal motor nucleus; X, vagal motor nucleus.

recordings (n = 6 cells, n = 6 preparations). A Vibratome cut was made dorsal to the pTRG to gain a better access to the cells. The recorded neurons displayed clear depolarizing currents in phase with the spontaneous respiratory activity (Fig. 4*A*). Electrical stimulation of the MLR induced short-latency EPSCs (7.8 ± 3.3 ms) that followed high-frequency stimulation (16 Hz; Fig. 4*B*), compatible with a monosynaptic connection in lampreys (42). In five preparations tested, bath application of CNQX and AP5 greatly reduced the EPSCs (76.9% ± 20.7% reductions; one-tailed paired t test; n = 5 pTRG neurons; $P < 0.001$; Fig. 4*C*), and a partial recovery was obtained after washout in four cases (57.9 ± 17.1% of control; one-tailed paired t test; n = 4 pTRG neurons;

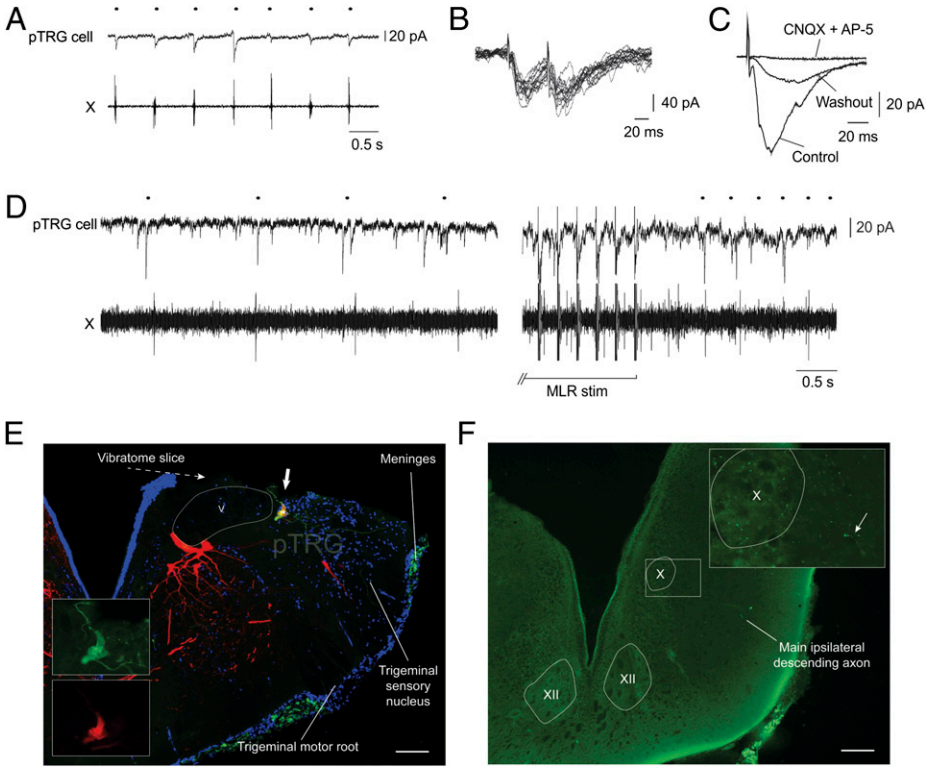

Fig. 4. Electrophysiological and anatomical characterization of pTRG premotor respiratory interneurons. (*A*) Voltage-clamp whole-cell recording of a neuron in the respiratory generator (i.e., pTRG). The neuron was retrogradely labeled from the IX respiratory motor nucleus. Excitatory currents occurred in-phase with respiratory activity recorded extracellularly from the vagal nucleus (X). (*B*) EPSCs induced by high-frequency (16 Hz) electrical stimulation of the MLR in a pTRG neuron. (*C*) Effect of a bath application of CNQX (50 μM) and AP5 (100 μM) on the MLR-induced EPSCs. (*D*) Electrical stimulation of the MLR induces excitatory currents and an increase of baseline currents in a pTRG interneuron, along with an increase of respiratory activity. (*E*) Superimposition of three photomicrographs of the recorded pTRG neuron filled with biocytin (green) and retrogradely filled from an injection of dextran amines (red) in the IX nucleus. DAPI labeling (blue) shows the location of DNA-containing cell nuclei. (Scale bar: 100 μm.) (*F*) Photomicrograph illustrating an axonal branch of the pTRG cell (arrow) in the ipsilateral X motor nucleus in the caudal brainstem. (Scale bar: 100 μm.) Dots indicate respiratory bursts. V, trigeminal motor nucleus; X, vagal motor nucleus; XII, hypoglossal motor nucleus.

$P < 0.01$ with effect, $P < 0.05$ with control). It is noteworthy that the bath application of CNQX and AP5 also abolished respiratory activity. In normal Ringer solution, when stimulating the MLR (1–10 μA; 3–5 Hz; 2-ms pulse duration; 10 s), the increases in frequency were present both in the pTRG cell and the respiratory motoneurons (Fig. 4*D*). The respiratory activity was generally weaker and slower in these preparations, presumably because of the Vibratome cut performed above the pTRG. Injection of the recorded pTRG cells with intracellular dye revealed descending axonal branches with varicosities in the respiratory motoneuron pools (Fig. 4 *E* and *F*). Altogether, these experiments suggest that MLR neurons send monosynaptic glutamatergic inputs to respiratory pTRG neurons that in turn project to respiratory motoneurons. The anatomical findings suggest that a dorsal subpopulation of MLR cells could be involved in the modulation of respiration, whereas more ventral MLR cells project to reticulospinal cells that are involved in the control of locomotion.

Role of Dorsal MLR in Respiratory Changes Associated with Locomotion. We have further examined the role of MLR neurons in modulating respiratory activity during active locomotion. Experiments were performed on semi-intact lampreys in which the brain and rostral spinal cord were first exposed and then the rostral forebrain removed, while the tail was left intact and free to swim in a deeper part of the bath ($n = 5$ preparations; Fig. 5*A*). In this preparation, stimulation of the PT (5–10 μA; 3–5 Hz; 2-ms pulse duration; 10 s) induced swimming that was associated with increases in respiratory activity (increases of 77.2 ± 56.5%; Wilcoxon signed-rank test, $P < 0.001$; $n = 15$ locomotor bouts; Fig. 5 *B*, *C*, *F*, and *G*, red). Local injections of CNQX (1 mM) and AP5 (500 μM) were then performed in the dorsal part of the MLR to test whether this area was involved in the respiratory increase. The injections considerably reduced the respiratory increases associated with locomotion (increases of 16.9 ± 25.7%; Wilcoxon signed-rank test, $P < 0.05$ for the increases; Mann–Whitney rank-sum test, $P < 0.01$ for difference with increases in control; Fig. 5 *D–F*, blue). The frequency of swimming was not significantly changed after the injection (2.63 ± 1.71 Hz in control vs. 2.00 ± 1.31 Hz after injection; Mann–Whitney rank-sum test, $P = 0.44$; $n = 15$ locomotor bouts in control, $n = 6$ locomotor bouts after injection; comparison made at time 0–15 s; Fig. 5*G*). To further support the contribution of MLR cell bodies in the respiratory effects and to determine whether they were sensitive to GABA, we also performed MLR stimulation with D-glutamate while applying GABA in the dorsal part of the MLR. The GABA injections considerably reduced the respiratory effects ($n = 5$ preparations; Fig. S6). These experiments show that a major part of the respiratory increases linked to movement rely on a specific dorsal region of the MLR and that blockade of this region affects respiratory activity without modifying locomotor activity.

Discussion

How respiration is modified to compensate for an increased energy demand during movement and exercise has been an important question in physiology that was investigated during the past century. Several lines of evidence have pointed to central

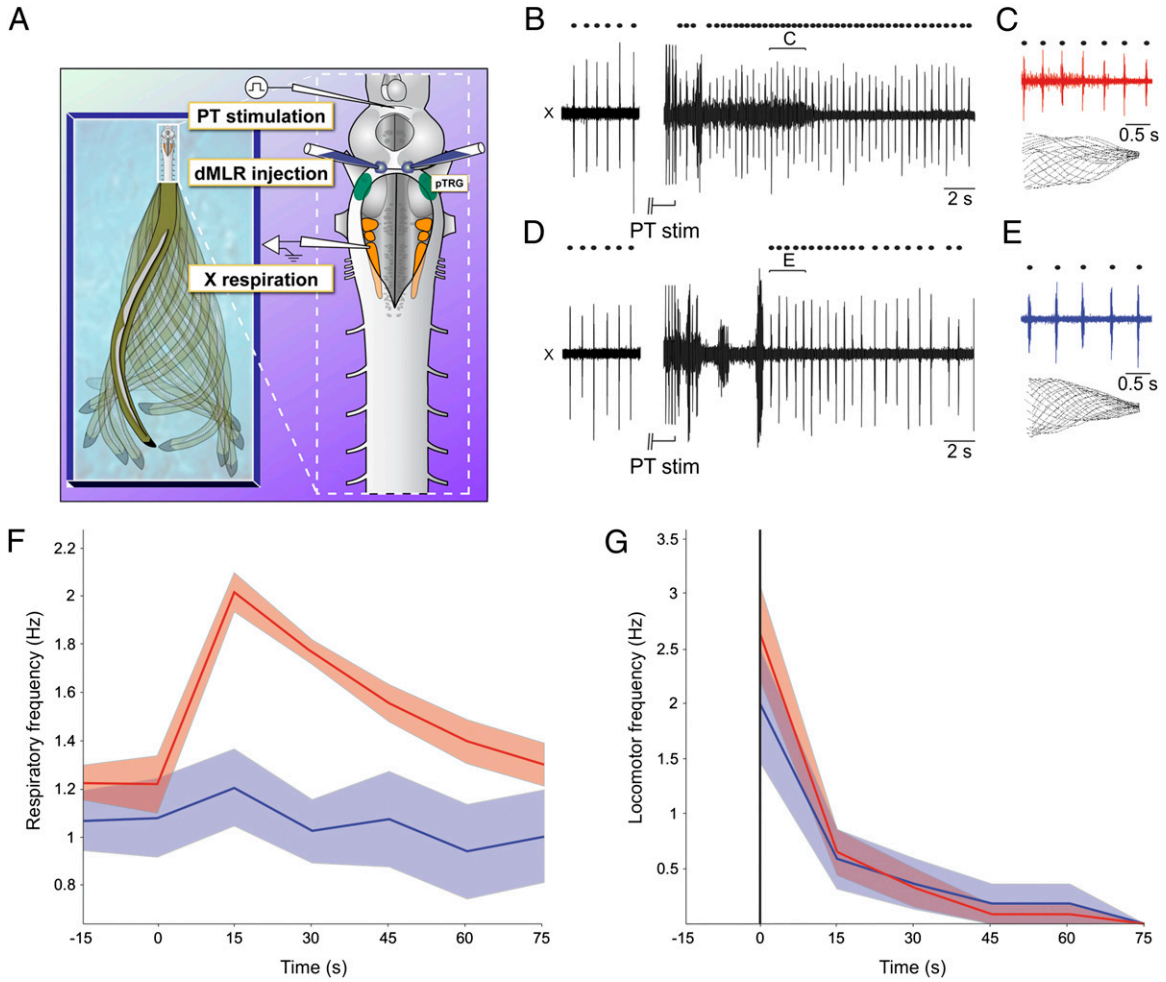

Fig. 5. Role of the dorsal MLR in respiratory modulation during locomotion. (*A*) Schematic representation of the semi-intact preparation. (*B*) Respiratory increases following PT stimulation that induced locomotor movements. (*C*) Close-up of the respiratory bursts during locomotion (*Upper*) and drawings of tail movements induced by the PT stimulation (*Lower*). (*D*) Respiratory increase following PT stimulation after blockade of the dorsal part of the MLR (dMLR) with microinjections of CNQX (1 mM) and AP5 (500 μM). (*E*) Close-up of the respiratory bursts during locomotion (*Upper*) and drawings of tail movements induced by the PT stimulation (*Lower*). (*F*) Analysis of all PT stimulation in all lampreys (n = 5 preparations) in control situation (blue, n = 15) and after blockade of the dorsal part of the MLR (red, n = 6). Data were triggered around the beginning of locomotion (i.e., time 0) and were pooled in classes of 15 s. The shaded area around the curves corresponds to the SE of the mean. (*G*) Similar analysis for locomotor frequency. Dots indicate respiratory bursts. PT, posterior tuberculum; X, vagal motor nucleus.

neural connections as possible mechanisms (12–14), but the hypothesized neural connections were never identified. In this study, we show that a group of neurons dorsally located in the MLR sends direct inputs to pTRG neurons. Moreover, blocking excitatory synaptic transmission in the dorsal part of the MLR greatly reduces the respiratory increases associated with locomotion, despite the presence of active locomotor movements.

Monosynaptic Connections from MLR Neurons to Neurons in Respiratory Generator. In this study, we provide several lines of evidence indicating that the MLR projects to the respiratory CPG. MLR stimulation increases respiratory frequency and resets the respiratory rhythm. As shown for other systems such as locomotor networks (43), this indicates that the CPG receives direct or indirect inputs from the stimulated region. We have identified a population of MLR neurons with direct projections to the pTRG and respiratory motoneurons by using retrograde labeling. Projections from the MLR to cranial motor nuclei including some with respiratory functions were proposed to exist in cats and rats (44, 45), but direct connections to neurons in the respiratory generator remained to be identified. Interestingly, the MLR neurons projecting to respiratory areas did not project to the locomotor areas, as would be expected if the same neurons would control respiration and locomotion in parallel. Therefore, our results suggest that respiration is controlled by a subpopulation of cells in the dorsal MLR. The fact that we could abolish a major part of the respiratory increase without affecting the locomotor pattern by blocking the dorsal part of the MLR also supports the idea that the MLR neurons controlling respiration and locomotion constitute separate populations. We also show that the population of dorsal MLR cells possess bilateral projections to the pTRG and respiratory motoneurons. This could contribute to the bilateral synchronization of the respiratory rhythm, which was shown to rely on crossing hindbrain respiratory neurons in mammals (46).

Functional Significance. It is well documented that respiration increases before and during movement in many animal species, including humans, and that the respiratory changes are correlated to the intensity of the muscular effort (1, 2, 8, 10, 12–14). Classically, the fast respiratory response to exercise was thought to result from a neural component, whereas the late respiratory changes were thought to result from combined neural and pe-

ripheral components (1). In this study, we describe a direct connection between the MLR and the respiratory generator that could underlie both the early and late respiratory changes. Indeed, we found that blocking excitatory transmission in the dorsal MLR markedly reduced not only the early changes but changes throughout the locomotor bout. Moreover, the neural substrate we describe in the present study does not require sensory inputs to activate the respiratory centers, nor does it require the spinal cord, caudal part of the hindbrain, or forebrain. Because the MLR initiates locomotion and controls the intensity of the locomotor output (36, 47), MLR neurons are presumed to encode information on the intended locomotor activity before it is relayed to the reticulospinal cells. This would make these neurons good candidates to adjust respiration before the movement is executed. This does not preclude possible additional contributions from sensory inputs to the respiratory adjustments. However, it is tempting to speculate that modifying respiration through direct projections from a brainstem center controlling locomotion could provide an advantage in terms of speed and precision of the respiratory increases. Other cells than those identified using single-cell recordings might be present in the dorsal MLR and might participate in the respiratory changes through other mechanisms than direct glutamatergic projections. However, whole-cell recording of neurons in the pTRG allowed us to show that most of the excitatory inputs from the MLR to these neurons are of very short latency and are abolished by glutamatergic receptor blockers.

It was proposed that the central command modifying respiration during exercise originated from the cerebral cortex (1, 48, 49) or the hypothalamus (12). Forebrain structures project directly or indirectly to the MLR (50). One possibility raised by the present study is that upstream locomotor centers could use the MLR as a relay to increase respiration during locomotion. We show that MLR cells are activated by stimulation of the PT, thought to be homologous to the substantia nigra of amniotes (51). We also show that blocking the dorsal part of the MLR while stimulating the PT nearly abolishes the respiratory increase associated with locomotion. This suggests that higher centers might necessitate the dorsal MLR to exert their respiratory effect. It was recently shown that the lamprey possesses important parts of the basal ganglia circuitry that is present in mammals (52). A better understanding of the interconnections between this circuitry and the MLR neurons might shed light on how higher motor centers control multiple behaviors in parallel.

It is well documented that mental simulation of physical effort and preparation for effort in humans induce respiratory and heart rate increases (10, 11). Furthermore, it was shown by using functional MRI that the MLR is activated in human subjects in similar tasks (40). The respiratory changes following mental simulation of movement were proposed to result from the activation of specialized motor anticipation networks or from components of the normal motor control regions (53). Our results provide support to the latter view because respiratory changes clearly occurred upon stimulation of the MLR at subthreshold levels. Hypothetically, the MLR neurons responsible for the respiratory command might be activated earlier than those controlling locomotion. This is supported by the observation that the recorded MLR neurons displayed excitation several seconds before the onset of MRRN activity, known to be part of the locomotor command signal reaching the spinal cord to generate locomotion (54).

Rethinking the Role of MLR. The MLR has been traditionally described as a region receiving convergent inputs from higher brain regions. It was believed to integrate these inputs to induce and control locomotion by providing excitation to reticulospinal cells in the lower brainstem (36–38, 54, 55). Other studies showed that stimulating locomotor centers induces increases in respiratory activity (12–14), but it was not known whether the respiratory effect was induced directly by MLR neurons or by a feedback from the spinal cord and caudal brainstem. Our results now show that the MLR contains a set of neurons with specific projections to the respiratory centers, and that this pathway increases respiration in the absence of the caudal brainstem and the spinal cord networks controlling locomotion. Another example of the divergent outputs of the MLR is the recently described parallel projection to a group of muscarinoceptive cells at the pontobulbar border, which increases the locomotor output (56). Thus, the view that emerges from recent studies, including the present study, is that MLR neurons transform locomotor commands coming from higher brain areas into multifunctional outputs controlling respiration and locomotion through independent subsets of neurons. This view also provides an interesting addition to an ongoing discussion about regional specificity in the brain. Basic motor and sensory functions are often believed to originate from highly specialized regions (57). Our results, on the contrary, indicate that the MLR, rather than being highly specialized in a single motor function, controls multiple functions with a common high-level goal: to allow animals to move in their environment while maintaining respiratory homeostasis.

Materials and Methods

All surgical and experimental procedures conformed to the guidelines of the Canadian Council on Animal Care and were approved by the animal care and use committee of the Université de Montréal and the Université du Québec à Montréal. Care was taken to minimize the number of animals used and their suffering. Experiments were performed on 102 postmetamorphic and spawning-phase adult sea lampreys, *Petromyzon marinus*, that were collected from the Great Chazy river (New York), Lake Huron (Ontario, Canada), and Morpion Stream (Ste-Sabine, QC, Canada). Some postmetamorphic animals were purchased from ACME Lamprey (Maine). The animals were kept in aerated water at 7 °C.

In Vitro Animal Preparation. For patch recording experiments, a surgery was made 24 h preceding the experiment to inject Texas red–dextran amines in the IX nucleus in vivo. This was done by anesthetizing the animals in tricaine methanesulfonate (MS 222, 100 mg/L of fresh water) and then transferring the animal in cold oxygenated Ringer solution (8–10 °C, 100% O_2) of the following composition (in mM): 130 NaCl, 2.1 KCl, 2.6 $CaCl_2$, 1.8 $MgCl_2$, 4 Hepes, 4 dextrose, and 1 $NaHCO_3$ (pH 7.4). A 2-mm^2 flap window was opened on the top of the head to expose the caudal brainstem. Needles were introduced in the IX nucleus to inject crystals of the dye. The incision was closed with Vetbond after the injection procedure. The animal was then returned to a small nursery aquarium filled with oxygenated Ringer solution for the night at room temperature. This injection was designed to retrogradely label both the population of MLR and pTRG neurons projecting to the respiratory motoneurons.

For electrophysiological experiments, the animals were first anesthetized and transferred into Ringer solution as described earlier. A complete transverse section was then performed approximately 2 cm caudal to the seventh gill pore, leaving approximately 15 myotomal segments (among ~100). The viscera and muscles were dissected out. The brain and spinal cord were exposed on their dorsal surface. The preparation was then pinned down onto silicone elastomer (Sylgard) at the bottom of an experimental chamber continually perfused with cold Ringer solution at a rate of approximately 4 mL/min. The cranial nerves were cut proximally to the brain to abolish possible sensory feedback. The brain tissue rostral to the mesencephalon was removed, except for experiments in which we stimulated the PT. In some experiments, a transverse section was made at the obex to isolate the brainstem from the spinal cord. To access the pTRG and MLR cells with patch electrodes, a Vibratome cut of the dorsal tissue of the pons and mesencephalon was performed in cold Ringer solution (1–3 °C). For MLR cell recordings, only the optic tectum and the dorsal isthmic region were removed. For pTRG cell recordings, the alar plate lateral to the V nucleus, the dorsal part of the V motor nucleus, the dorsal isthmic region, and the optic tectum were removed.

Electrophysiological Experiments. Extracellular recordings of spinal ventral roots, respiratory motoneurons, and the pTRG were made by using glass electrodes filled with Ringer solution (tip diameter ~5 μm) and connected to

a microelectrode AC amplifier (low cutoff, 100 Hz; high cutoff, 500 Hz; model 1800; A-M Systems; Fig. S1).

Respiratory motoneurons were recorded intracellularly with sharp glass microelectrodes (4 M KAc; 80–120 MΩ). The signals were amplified through an Axoclamp 2A amplifier (sampling rate, 10 kHz; Axon Instruments). The motoneurons were impaled by directing the tip of the electrode to the IX or the rostral X motor nucleus. Motoneurons always displayed rhythmical membrane potential oscillations that were synchronous with the respiratory output recorded from the motoneuronal pools with extracellular electrodes. Patch recordings of pTRG and MLR cells were made in whole-cell voltage-clamp mode (−60 to −70 mV) with a model 2400 amplifier (A-M Systems). The cells were targeted under an Eclipse FN-1 microscope (Nikon Instruments) equipped for fluorescence. Patch pipette solution contained (in mM) cesium methane sulfonate 102.5, NaCl 1, $MgCl_2$ 1, EGTA 5, and Hepes 5, and 0.1% biocytin. pH was adjusted to 7.2 with CsOH, and pipettes were pulled to a tip resistance of 5 MΩ.

The MLR was stimulated chemically or electrically. The PT was stimulated electrically. Chemical stimulation was performed by pressure-injecting the excitatory amino acid D-glutamate (2.5 mM; Sigma), diluted in Ringer solution at pH 7.4 through a glass micropipette using a Picospritzer (General Valve). The inactive dye, fast green, was added to the drug solution to visually monitor the size and exact location of the injections. In some experiments, the same equipment was used to inject the ionotropic glutamatergic receptor blockers CNQX (1 mM) and AP5 (500 μM) in the pTRG and in other brainstem sites. The size of the pTRG and MLR injections was assessed visually by measuring the spread of the dye, fast green, in the tissue with a dissecting microscope equipped with a calibrated ocular micrometer. The spread was less than 300 μm in diameter for those injections. Theoretically, the maximal injection volume can be estimated by using the equation that links the volume of a sphere to its diameter. As such, the maximal volume of these injections would be 14 nL. Bath application of CNQX (50 μM) and AP5 (100 μM) were also performed. After each D-glutamate injection in the MLR, a washout period was allowed for recovery (several minutes to >1 h). To obtain subthreshold effects on respiration (i.e., respiratory effects without locomotion), the MLR was first localized by performing injections that resulted in fictive locomotion. The Picospritzer pressure was then reduced to a level that remained subthreshold for inducing fictive locomotion. The spread of these injections was less than 50 μm in diameter. Based on the equation as described earlier, the maximal volume of these injections would be 0.1 nL. The spread of the dorsal MLR injections was also less than 50 μm in diameter (Fig. 5 and Fig. S6).

Electrical stimulation of the MLR and PT was performed with glass-coated tungsten microelectrodes (0.8–2 MΩ). For experiments in which the spinal cord was removed, the activity of reticulospinal cells in the brainstem was monitored before and after the spinal cord lesion by using an extracellular electrode to verify that the effects of MLR stimulation on the locomotor networks were still present. The stimulation site (i.e., MLR) was marked by an electrolytic lesion made by passing a continuous negative current of 5 μA during 10 s in 16 preparations in which we measured electrically induced locomotion, respiratory rhythm resetting, and motoneuronal EPSPs in response to MLR stimulation.

Semi-intact preparations were used to apply electrophysiological techniques in the brainstem while observing active locomotor movements from the intact tail (Fig. 5). For this preparation, we dissected the brainstem similarly to the in vitro preparation, but the spinal cord and tail were left intact and free to swim in a deeper part of the bath. The locomotor movements were analyzed using the same technique that was used for in vivo recordings (*SI Materials and Methods*).

Data Acquisition and Analyses. Data were acquired via a Digidata 1322A interface by using Clampex 9 software (Axon Instruments) for computer analysis. Respiratory and locomotor bursts were detected and analyzed by using homemade software. The instantaneous frequency of the respiratory activity was calculated as the inverse of the time interval between the beginnings of two consecutive respiratory bursts. The area was measured on a rectified and filtered version of the signal (root mean square, 10-ms bins). The area of the respiratory bursts, EPSPs, and EPSCs was normalized because of the variability between preparations. This normalization was obtained by multiplying values of area by 100 and dividing by the average measure in control situation for each individual lamprey.

The effects of MLR and PT stimulation on respiration were examined on 20 respiratory cycles before (i.e., control) and during fictive locomotion. The duration of the effect on frequency and area of the respiratory bursts was analyzed by using iterated *t* tests between a group of 20 control bursts and a moving window of 20 bursts after the stimulation. For in vivo experiments, anticipatory respiratory changes were characterized by comparing the frequency of respiratory bursts occurring during a window of 6 s preceding any movement with a set of bursts occurring at rest, more than 10 s before the beginning of locomotion. For semi-intact preparations, respiratory frequencies were regrouped in classes of 15 s (i.e., 0–15 s, 15–30 s) and triggered on locomotion onset to facilitate the pooling of data from multiple preparations.

EPSPs and EPSCs were analyzed using Spike2 version 5.19 (Cambridge Electronic Design) and homemade scripts. The area under the curve was measured from the end of the stimulation artifact to the end of the EPSPs.

Data in the text are given as means ± SD unless specified otherwise. Data in Fig. 5 are given as mean ± SEM. Statistical analyses were carried out using Origin (OriginLab) or SigmaStat version 3.5 (Systat). A Student *t* test was used to compare the means of two groups. The Wilcoxon and Mann–Whitney tests were used when the compared distributions did not respect the assumptions of normality of distributions or equality of variance. Distributions were considered statistically significant when the value of *P* was lower than 0.05.

Histology and Axonal Tracing Experiments. Details of the histological procedures were published elsewhere (36, 41) and are provided in *SI Materials and Methods*. Electrophysiological and anatomical figures were designed using CorelDraw 4 software (Corel). The projections of all of the intracellularly labeled cells were examined in details from serial sections. One MLR neuron was reconstructed in 3D for illustrative purposes by using Neurolucida (MBF Neuroscience; Fig. 3). In the 3D model, the contours of the brainstem; MRRN; posterior rhombencephalic reticular nucleus; V, VII, IX, and X motor nuclei; and pTRG were first outlined on each cross-section.

ACKNOWLEDGMENTS. The authors thank Danielle Veilleux for her technical assistance, Christian Valiquette for his skillful programming of data analysis software, and Frédéric Bernard for his help with the graphics and the figures; Dr. Roger Bergstedt, William D. Swink, and Mary K. Jones from the Lake Huron Biological Station in Michigan, Brad Young and Wayne Bouffard from the US Fish and Wildlife Service of Vermont, and R. McDonald from the Sea Lamprey Control Center in Sault Ste. Marie, ON, Canada, for their kind supply of lampreys; and Laurent Juvin, Dimitri Ryczko, and Karine Fénelon for their comments on the manuscript. This work was supported by Natural Sciences and Engineering Research Council of Canada Grant 217435 (to R.D.), Canadian Institutes of Health Research (CIHR) Grants 15129 (to R.D.) and 84765 (to J.-F.G.), Great Lake Fisheries Commission Grant 8400272, and Fonds de la Recherche en Santé du Québec (FRSQ) Group Grant 5249. J.-F.G. received studentships from the FRSQ and the Canadian Institutes of Health Research.

1. Dejours P, Raynaud J, Cuénod CL, Labrousse Y (1955) Modifications instantanées de la ventilation au début et à l'arrêt de l'exercice musculaire. Interprétation. *J Physiol (Paris)* 47:155–159.
2. Mateika JH, Duffin J (1995) A review of the control of breathing during exercise. *Eur J Appl Physiol Occup Physiol* 71:1–27.
3. Scott K (2011) Out of thin air: Sensory detection of oxygen and carbon dioxide. *Neuron* 69:194–202.
4. Gestreau C, et al. (2010) Task2 potassium channels set central respiratory CO2 and O2 sensitivity. *Proc Natl Acad Sci USA* 107:2325–2330.
5. Gourine AV, et al. (2010) Astrocytes control breathing through pH-dependent release of ATP. *Science* 329:571–575.
6. Lipton AJ, et al. (2001) S-nitrosothiols signal the ventilatory response to hypoxia. *Nature* 413:171–174.
7. Gariépy JF, Missaghi K, Dubuc R (2010) The interactions between locomotion and respiration. *Prog Brain Res* 187:173–188.
8. Bramble DM, Carrier DR (1983) Running and breathing in mammals. *Science* 219: 251–256.
9. Morin D, Viala D (2002) Coordinations of locomotor and respiratory rhythms in vitro are critically dependent on hindlimb sensory inputs. *J Neurosci* 22:4756–4765.
10. Tobin MJ, Perez W, Guenther SM, D'Alonzo G, Dantzker DR (1986) Breathing pattern and metabolic behavior during anticipation of exercise. *J Appl Physiol* 60: 1306–1312.
11. Decety J, Jeannerod M, Durozard D, Baverel G (1993) Central activation of autonomic effectors during mental simulation of motor actions in man. *J Physiol* 461:549–563.
12. Eldridge FL, Millhorn DE, Waldrop TG (1981) Exercise hyperpnea and locomotion: parallel activation from the hypothalamus. *Science* 211:844–846.
13. DiMarco AF, Romaniuk JR, Von Euler C, Yamamoto Y (1983) Immediate changes in ventilation and respiratory pattern associated with onset and cessation of locomotion in the cat. *J Physiol* 343:1–16.
14. Kawahara K, Nakazono Y, Yamauchi Y, Miyamoto Y (1989) Coupling between respiratory and locomotor rhythms during fictive locomotion in decerebrate cats. *Neurosci Lett* 103:326–330.
15. Waldrop TG, Iwamoto GA (2006) Point: Supraspinal locomotor centers do contribute significantly to the hyperpnea of dynamic exercise. *J Appl Physiol* 100:1077–1079.

16. Waldrop TG, Iwamoto GA (2006) Point: Supraspinal locomotor centers do contribute significantly to the hyperpnea of dynamic exercise. *J Appl Physiol* 100:1077–1079.
17. Del Negro CA, Morgado-Valle C, Feldman JL (2002) Respiratory rhythm: An emergent network property? *Neuron* 34:821–830.
18. Paton JF, Abdala AP, Koizumi H, Smith JC, St-John WM (2006) Respiratory rhythm generation during gasping depends on persistent sodium current. *Nat Neurosci* 9: 311–313.
19. Pace RW, Mackay DD, Feldman JL, Del Negro CA (2007) Inspiratory bursts in the preBötzinger complex depend on a calcium-activated non-specific cation current linked to glutamate receptors in neonatal mice. *J Physiol* 582:113–125.
20. Wittmeier S, Song G, Duffin J, Poon CS (2008) Pacemakers handshake synchronization mechanism of mammalian respiratory rhythmogenesis. *Proc Natl Acad Sci USA* 105: 18000–18005.
21. Tan W, et al. (2008) Silencing preBötzinger complex somatostatin-expressing neurons induces persistent apnea in awake rat. *Nat Neurosci* 11:538–540.
22. Rose MF, Ahmad KA, Thaller C, Zoghbi HY (2009) Excitatory neurons of the proprioceptive, interoceptive, and arousal hindbrain networks share a developmental requirement for Math1. *Proc Natl Acad Sci USA* 106:22462–22467.
23. Rose MF, et al. (2009) Math1 is essential for the development of hindbrain neurons critical for perinatal breathing. *Neuron* 64:341–354.
24. Rubin JE, Hayes JA, Mendenhall JL, Del Negro CA (2009) Calcium-activated nonspecific cation current and synaptic depression promote network-dependent burst oscillations. *Proc Natl Acad Sci USA* 106:2939–2944.
25. Thoby-Brisson M, et al. (2009) Genetic identification of an embryonic parafacial oscillator coupling to the preBötzinger complex. *Nat Neurosci* 12:1028–1035.
26. Hägglund M, Borgius L, Dougherty KJ, Kiehn O (2010) Activation of groups of excitatory neurons in the mammalian spinal cord or hindbrain evokes locomotion. *Nat Neurosci* 13:246–252.
27. Williams RH, Burdakov D (2008) Hypothalamic orexins/hypocretins as regulators of breathing. *Expert Rev Mol Med* 10:e28.
28. Ptak K, et al. (2009) Raphé neurons stimulate respiratory circuit activity by multiple mechanisms via endogenously released serotonin and substance P. *J Neurosci* 29: 3720–3737.
29. Doi A, Ramirez JM (2010) State-dependent interactions between excitatory neuromodulators in the neuronal control of breathing. *J Neurosci* 30:8251–8262.
30. Smith JC, Ellenberger HH, Ballanyi K, Richter DW, Feldman JL (1991) Pre-Bötzinger complex: A brainstem region that may generate respiratory rhythm in mammals. *Science* 254:726–729.
31. Feldman JL, Del Negro CA (2006) Looking for inspiration: New perspectives on respiratory rhythm. *Nat Rev Neurosci* 7:232–242.
32. Martel B, et al. (2007) Respiratory rhythms generated in the lamprey rhombencephalon. *Neuroscience* 148:279–293.
33. Mutolo D, Bongianni F, Einum J, Dubuc R, Pantaleo T (2007) Opioid-induced depression in the lamprey respiratory network. *Neuroscience* 150:720–729.
34. Mutolo D, Bongianni F, Cinelli E, Pantaleo T (2010) Role of neurokinin receptors and ionic mechanisms within the respiratory network of the lamprey. *Neuroscience* 169: 1136–1149.
35. Mutolo D, Cinelli E, Bongianni F, Pantaleo T (2011) Identification of a cholinergic modulatory and rhythmogenic mechanism within the lamprey respiratory network. *J Neurosci* 31:13323–13332.
36. Sirota MG, Di Prisco GV, Dubuc R (2000) Stimulation of the mesencephalic locomotor region elicits controlled swimming in semi-intact lampreys. *Eur J Neurosci* 12: 4081–4092.
37. Grillner S (2006) Biological pattern generation: The cellular and computational logic of networks in motion. *Neuron* 52:751–766.
38. Grillner S, Wallén P, Saitoh K, Kozlov A, Robertson B (2008) Neural bases of goal-directed locomotion in vertebrates–an overview. *Brain Res Brain Res Rev* 57:2–12.
39. Shik ML, Severin FV, Orlovskiĭ GN (1966) [Control of walking and running by means of electric stimulation of the midbrain]. *Biofizika* 11:659–666.
40. Jahn K, et al. (2008) Imaging human supraspinal locomotor centers in brainstem and cerebellum. *Neuroimage* 39:786–792.
41. Derjean D, et al. (2010) A novel neural substrate for the transformation of olfactory inputs into motor output. *PLoS Biol* 8:e1000567.
42. Brocard F, Dubuc R (2003) Differential contribution of reticulospinal cells to the control of locomotion induced by the mesencephalic locomotor region. *J Neurophysiol* 90: 1714–1727.
43. Conway BA, Hultborn H, Kiehn O (1987) Proprioceptive input resets central locomotor rhythm in the spinal cat. *Exp Brain Res* 68:643–656.
44. Edwards SB (1975) Autoradiographic studies of the projections of the midbrain reticular formation: descending projections of nucleus cuneiformis. *J Comp Neurol* 161:341–358.
45. Grofova I, Keane S (1991) Descending brainstem projections of the pedunculopontine tegmental nucleus in the rat. *Anat Embryol (Berl)* 184:275–290.
46. Bouvier J, et al. (2010) Hindbrain interneurons and axon guidance signaling critical for breathing. *Nat Neurosci* 13:1066–1074.
47. Dubuc R (2009) Locomotor regions in the midbrain (MLR) and diencephalon (DLR). *The Encyclopedia of Neuroscience*, eds Binder MD, Hirokawa N, Windhorst U (Springer, New York), pp 2168–2171.
48. Thornton JM, et al. (2001) Identification of higher brain centres that may encode the cardiorespiratory response to exercise in humans. *J Physiol* 533:823–836.
49. Krogh A, Lindhard J (1913) The regulation of respiration and circulation during the initial stages of muscular work. *J Physiol* 47:112–136.
50. Jordan LM (1998) Initiation of locomotion in mammals. *Ann N Y Acad Sci* 860:83–93.
51. Pombal MA, El Manira A, Grillner S (1997) Afferents of the lamprey striatum with special reference to the dopaminergic system: A combined tracing and immunohistochemical study. *J Comp Neurol* 386:71–91.
52. Stephenson-Jones M, Samuelsson E, Ericsson J, Robertson B, Grillner S (2011) Evolutionary conservation of the basal ganglia as a common vertebrate mechanism for action selection. *Curr Biol* 21:1081–1091.
53. Oishi K, Kasai T, Maeshima T (2000) Autonomic response specificity during motor imagery. *J Physiol Anthropol Appl Human Sci* 19:255–261.
54. Antri M, Fénelon K, Dubuc R (2009) The contribution of synaptic inputs to sustained depolarizations in reticulospinal neurons. *J Neurosci* 29:1140–1151.
55. Dubuc R, et al. (2008) Initiation of locomotion in lampreys. *Brain Res Brain Res Rev* 57: 172–182.
56. Smetana R, Juvin L, Dubuc R, Alford S (2010) A parallel cholinergic brainstem pathway for enhancing locomotor drive. *Nat Neurosci* 13:731–738.
57. Kanwisher N (2010) Functional specificity in the human brain: A window into the functional architecture of the mind. *Proc Natl Acad Sci USA* 107:11163–11170.